

Recent Results from Long-Baseline Neutrino Experiments

ALYSIA D. MARINO

Department of Physics

University of Colorado Boulder, UCB 390 , Boulder CO, 80309, USA

We are moving into an era of precision measurements of neutrino mixing, and it is increasingly necessary to use a 3-flavor framework to describe the results. This paper will focus on recent results from long-baseline neutrino experiments, especially accelerator-based beams. Using ν_μ beams, we have now observed the disappearance of ν_μ , and the appearance of both ν_e and ν_τ . It will also briefly describe some of the long-baseline experiments that have recently started operation, from which data are expected soon.

PRESENTED AT

XXXIV Physics in Collision Symposium
Bloomington, Indiana, September 16–20, 2014

1 Neutrino Mixing

Over the past 20 years, compelling evidence has emerged for neutrino flavor oscillations. This evidence has been seen over a wide range of energies and distances and with both natural and manmade neutrino sources.

We can interpret these results as arising from the fact that neutrinos are produced in flavor eigenstates of the weak interaction (ν_e , ν_μ , and ν_τ), and these are a mixture of neutrino mass eigenstates (ν_1 , ν_2 , and ν_3). Interference between the flavor eigenstates causes the apparent neutrino flavor to oscillate with distance. The mixing between the mass and flavor states can be well-described by a unitary mixing matrix, known as the MNSP matrix:

$$\begin{pmatrix} \nu_e \\ \nu_\mu \\ \nu_\tau \end{pmatrix} = \begin{pmatrix} U_{e1} & U_{e2} & U_{e3} \\ U_{\mu1} & U_{\mu2} & U_{\mu3} \\ U_{\tau1} & U_{\tau2} & U_{\tau3} \end{pmatrix} \begin{pmatrix} \nu_1 \\ \nu_2 \\ \nu_3 \end{pmatrix}. \quad (1)$$

In general, this mixing matrix can be parameterized as the product of three rotation matrices and a complex phase:

$$U = \begin{bmatrix} 1 & 0 & 0 \\ 0 & c_{23} & s_{23} \\ 0 & -s_{23} & c_{23} \end{bmatrix} \times \begin{bmatrix} c_{13} & 0 & s_{13}e^{-i\delta_{CP}} \\ 0 & 1 & 0 \\ -s_{13}e^{i\delta_{CP}} & 0 & c_{23} \end{bmatrix} \times \begin{bmatrix} c_{12} & s_{12} & 0 \\ -s_{12} & c_{12} & 0 \\ 0 & 0 & 1 \end{bmatrix} \quad (2)$$

where c_{ij} and s_{ij} are the cosines and sines of the three mixing angles θ_{12} , θ_{13} , and θ_{23} , and δ_{CP} is the phase. Anti-neutrinos mix via the complex conjugate of this matrix.

The probability to observe a neutrino transition from one flavor (α) to another (β) is given by [1]

$$P(\nu_\alpha \rightarrow \nu_\beta) = \delta_{\alpha\beta} - 4 \sum_{i>j} \Re(U_{\alpha i}^* U_{\beta i} U_{\alpha j} U_{\beta j}^*) \sin^2[\Delta m_{ij}^2(L/4E)] + 2 \sum_{i>j} \Im(U_{\alpha i}^* U_{\beta i} U_{\alpha j} U_{\beta j}^*) \sin[\Delta m_{ij}^2(L/2E)] \quad (3)$$

where L is the distance travelled, E is the neutrino energy, and Δm_{ij}^2 is the difference in the square of the neutrino masses $m_i^2 - m_j^2$. In this way, neutrino flavor change depends on the values of the three mixing angles, the differences between the three masses and the possible CP-violating phase δ_{CP} , all of which must be determined experimentally.

The oscillations are a function of $\Delta m^2 L/E$. For long-baseline neutrino beams, the oscillation effects are dominated by mixing between $\nu_1 - \nu_3$ and $\nu_2 - \nu_3$. It is known that Δm_{21}^2 is considerably smaller than Δm_{31}^2 , so for a ν_μ beam the mixing between $\nu_1 - \nu_2$ only becomes significant at very long distances or very low energies. The sign

of Δm_{31}^2 is currently unknown, thus we do not know if ν_3 is the heaviest neutrino (the so-called “normal hierarchy”) or the lightest neutrino (the “inverted hierarchy”)

For a beam of muon neutrinos, the survival probability for ν_μ is given approximately by

$$P(\nu_\mu \rightarrow \nu_\mu) \simeq 1 - \sin^2 2\theta_{23} \cdot \sin^2 (\Delta m_{32}^2 L/4E), \quad (4)$$

while appearance of ν_e in vacuum is

$$P(\nu_\mu \rightarrow \nu_e) \simeq \sin^2 2\theta_{13} \cdot \sin^2 \theta_{23} \cdot \sin^2 (\Delta m_{31}^2 L/4E). \quad (5)$$

Notice that the ν_e appearance depends on both the 1-3 and 2-3 sectors. As neutrinos travel through matter, Equation 5 is modified slightly to [2]

$$P(\nu_\mu \rightarrow \nu_e) \simeq \sin^2 2\theta_{13} \cdot \frac{\sin^2 \theta_{23}}{(A-1)^2} \cdot \sin^2 ((A-1)\Delta m_{31}^2 L/4E) \quad (6)$$

where $A = \sqrt{2}G_F N_e \frac{2E}{\Delta m_{31}^2}$, which depends on the Fermi coupling constant, G_F , and N_e , the electron number density of the material. Note that this expression depends on the sign of Δm_{31}^2 , and therefore on the neutrino mass hierarchy. A changes sign for anti-neutrinos, so even with a true $\delta_{CP} = 0$ the probability for $\nu_\mu \rightarrow \nu_e$ will be enhanced (suppressed) compared to $\bar{\nu}_\mu \rightarrow \bar{\nu}_e$ for the normal (inverted) hierarchy. Including the effects of non-zero δ_{CP} adds additional terms to $P(\nu_\mu \rightarrow \nu_e)$ including [2]

$$- \frac{|\Delta m_{21}^2| \sin \delta_{CP} \sin 2\theta_{12} \sin 2\theta_{13} \sin 2\theta_{23} \cos \theta_{13}}{|\Delta m_{31}^2| A(1-A)} \sin \Delta \sin (A\Delta) \sin ((1-A)\Delta), \quad (7)$$

where $\Delta = \Delta m_{31}^2 L/4E$. This term also changes sign for anti-neutrinos, but has a different dependence on L and E compared to the matter term in Equation 6. So in this way, differences between $\nu_\mu \rightarrow \nu_e$ and $\bar{\nu}_\mu \rightarrow \bar{\nu}_e$ can help to resolve the hierarchy question and provide a measurement of CP-violation in the lepton sector if δ_{CP} is found to be non-zero. Thus the interpretation of current and future neutrino beams will rely on using a 3-flavor description of neutrino oscillations and will focus on comparisons between neutrino and anti-neutrino signals.

2 MINOS Results

The Main Injector Neutrino Oscillation Search (MINOS) experiment [3] consists of two magnetized iron sampling calorimeters. The near detector has a mass of 1 kton and is located on the Fermilab site, approximately 1 km from the target. The far detector has a mass of 5.4 ktons and is 735 km away in the Soudan Mine in Minnesota. MINOS is located on the Neutrinos at the Main Injector (NuMI) neutrino beam, which

is initiated by 120 GeV protons. Two magnetic horns are used to focus the charged pions and kaons that result from the interactions of these protons in a graphite target. By changing the direction of the horn current, the beam can be either predominately ν_μ or $\bar{\nu}_\mu$.

MINOS collected data from May 2005 until May of 2012. A total of 10.7×10^{20} protons on target were collected with the beam in neutrino mode, while 3.61×10^{20} protons on target were collected in anti-neutrino mode. Additionally the far detector recorded 37.88 kton-years of atmospheric neutrino data.

MINOS recently published a combined 3-flavor fit to the beam neutrino and anti-neutrino data + atmospheric data [4]. This included a fit to both the ν_μ disappearance data and the ν_e appearance data. The value of θ_{13} was constrained by results from reactor neutrino experiments. The allowed regions are shown in Figure 1.

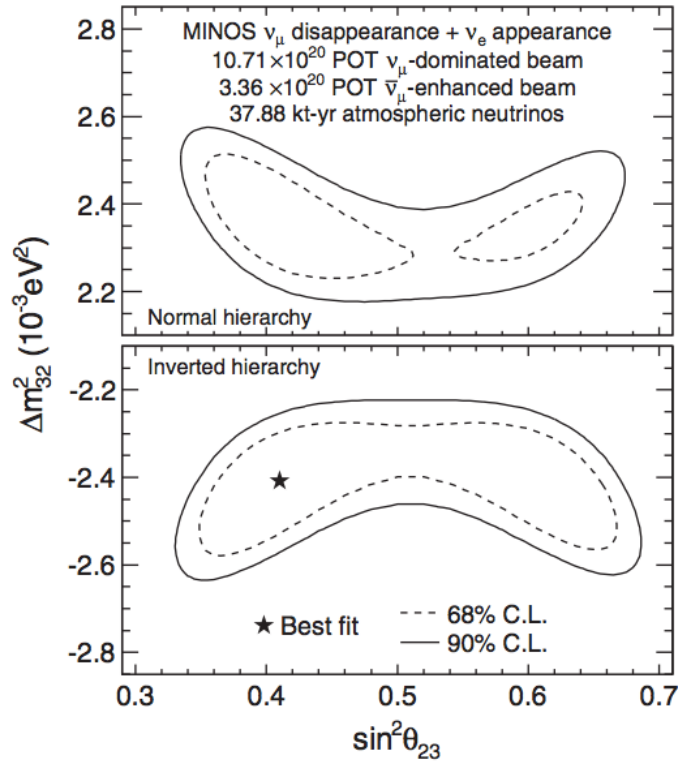


Figure 1: The allowed parameter regions are shown here at the 90% CL (solid) and 68% CL (dashed) from a combined fit to all of the MINOS data. Reproduced from [4].

MINOS has also directly compared the ν and $\bar{\nu}$ signals for both ν_μ [5] and ν_e [6]. For ν_μ disappearance, both have very similar best fit values and overlapping allowed regions. For ν_e the data somewhat disfavors negative values of δ_{CP} .

3 T2K Results

The Tokai-to-Kamioka (T2K) experiment [7] uses a beam that originates at the Japan Proton Accelerator Research Complex (J-PARC) on the east coast of Japan. T2K's ν_μ beam is initiated by 30 GeV protons striking a graphite target. Three magnetic horns focus the secondary hadrons. Near detectors are located 280 m from the target at J-PARC, while the Super-Kamiokande detector is used as the far detector, 295 km away. The beam is aimed 2.5° away from Super-Kamiokande and the off-axis near detector (ND280). This results in a beam with a narrower energy spectrum and enhanced flux at lower energies.

The ND280 near detector is magnetized. Its tracker consists of 2 fine-grained scintillator trackers sandwiched between 3 TPCs. A brass/lead/scintillator calorimeter forms a pi-zero detector, which sits upstream of the tracker. The detectors are surrounded by lead/scintillator electromagnetic calorimeters, and additional scintillator paddles are interspersed between the layers of the magnet yoke. One of the fine-grained scintillator detectors and the pi-zero detector also contain passive water targets. The far detector, Super-Kamiokande, is a water Cherenkov detector with a fiducial mass of 22.5 kton of water, surrounded by 11,000 phototubes. A separate veto detector surrounds the main detector to reject external events. As of October 2014, T2K has collected 6.88×10^{20} protons on target with the beam in neutrino mode. With the constraints on the flux and cross section from the ND280 and external data, the uncertainties on the number of expected ν_μ and ν_e events at SK are 7.7% and 6.8%, respectively.

T2K sees significant disappearance of ν_μ [9] and that currently yields the most precise measurement of θ_{23} . T2K also sees the appearance of ν_e [8] with a significance of 7.3σ compared to the background expectations without $\nu_\mu \rightarrow \nu_e$.

T2K has also recently performed a combined 3-flavor fit to both its ν_μ disappearance and ν_e appearance signals [10] in neutrino mode. Figure 2 compares the allowed regions for Δm_{23}^2 and $\sin^2 \theta_{23}$ from the T2K beam data, MINOS atmospheric ν and beam data, and Super-Kamiokande atmospheric ν data. The allowed regions from all three experiments agree very well. T2K has also performed this combined appearance/disappearance 3-flavor fit including a constraint on θ_{13} from reactor anti-neutrino disappearance searches. The $\Delta\chi^2$ for these fits as a function of δ_{CP} is shown in Figure 3. The data show a strong preference for negative values of δ_{CP} at the 90% CL.

In the summer of 2014 T2K also began collecting anti-neutrino data with 0.51×10^{20} protons on target collected so far. So far T2K has only collected $\simeq 10\%$ of its total proton on target goal, and future running will include a mixture of neutrino and anti-neutrino data.

4 Tau Appearance Results

Searches have also been conducted for $\nu_\mu \rightarrow \nu_\tau$. In [11] the OPERA experiment reported the detection of 3 ν_τ events in their 2008-2012 dataset. At the Neutrino 2014 conference they also reported a 4th ν_τ event so that the null oscillation hypothesis is now rejected at the 4.2σ confidence level.

Super-Kamiokande has also reported evidence for ν_τ appearance at the 3.8σ confidence level in atmospheric neutrino interactions that contain hadronic τ decays [12].

5 Near Future Projects

The MINOS experiment concluded in data taking 2012, however the detectors continue to operate in the NOvA-era NuMI beam as the MINOS+ experiment. Compared to the MINOS era, this beam has a higher power, a greater energy, and a greater flux of neutrinos per proton on target. The physics goals for MINOS+ include precision 3-flavor mixing tests, neutrino cross section measurements, and searches for sterile neutrinos and non-standard interactions.

The NOvA experiment uses the NuMI beam with highly-segmented active liquid scintillator detectors. In addition to a near detector at Fermilab, NOvA has a 14 kton far detector, located 810 km away in Ash River, Minnesota. Both detectors are approximately 14 mrad off of the axis of the beam. The first NOvA beam was delivered in 2013 and construction on both the near and far detectors was completed in 2014. The first physics results are expected within the next year.

With its longer baseline, the matter effects are more significant in NOvA than they are in T2K. For maximal θ_{23} mixing, NOvA can resolve the hierarchy at the 95% confidence level sensitivity over 1/3 of the range of δ_{CP} values, and the combination of NOvA and future T2K running can resolve the hierarchy at a significance that is better than 68% confidence over all possible values of δ_{CP} [14].

Future neutrino and anti-neutrino running with NOvA and T2K can constrain δ_{CP} [15]. Figure 4 shows the sensitivity to measuring non-zero δ_{CP} for T2K, NOvA, and the combined result. The combination of T2K and NOvA has more than 1σ sensitivity over 75% of the δ_{CP} range.

6 Conclusion

We are moving into an era of precision measurements of neutrino oscillation parameters with accelerator-based neutrino experiments. Increasingly it is necessary to use a 3-flavor framework to describe these oscillations.

In recent years MINOS and T2K have observed the disappearance of ν_μ and the appearance of ν_e . MINOS operations concluded in 2012, and they have reported a

joint 3-flavor analysis including both atmospheric neutrinos and beam neutrinos and anti-neutrinos. T2K has presented results using a neutrino beam, and the comparison of the T2K results to the results from reactor anti-neutrinos currently favors large negative values of δ_{CP} . The appearance of ν_τ has also been seen by the OPERA and Super-Kamiokande collaborations.

Our understanding of neutrino mixing will continue to improve over the next few years. T2K began collecting anti-neutrino data in the summer of 2014 and initial results are expected soon. MINOS+ and NOvA have started data collection and will also present their first physics results within the next year. These future results will dramatically increase knowledge of the neutrino mass hierarchy and leptonic CP violation.

References

- [1] B. Kayser, Proceedings of the SLAC Summer Institute on Particle Physics 2004, arXiv:hep-ph/0506165
- [2] K.A. Olive et al. (Particle Data Group), Chin. Phys. C, **38**, 090001 (2014).
- [3] D.G. Michael et al. (MINOS Collaboration), Nucl. Instrum.Meth. A **596** 190 (2008).
- [4] P. Adamson et al. (MINOS Collaboration), Phys. Rev. Lett., **112**, 191801 (2014).
- [5] P. Adamson et al. (MINOS Collaboration), Phys. Rev. Lett., **110**, 251801 (2013).
- [6] P. Adamson et al. (MINOS Collaboration), Phys. Rev. Lett., **110**, 171801 (2013).
- [7] K. Abe et al. (T2K Collaboration), Nucl. Instrum. Meth. A, **659**, 106 (2011).
- [8] K. Abe et al. (T2K Collaboration), Phys. Rev. Lett., **112** 061802 (2014).
- [9] K. Abe et al. (T2K Collaboration), Phys. Rev. Lett., **112** 181801 (2014).
- [10] C. Walter, “Results from T2K”, talk at the XXIVth International Conference on Neutrino Physics and Astrophysics (Neutrino 2014), June 2014.
- [11] N. Agafonova et al. (OPERA collaboration), Phys. Rev. D **89** 051102 (2014).
- [12] K. Abe et al. (Super-Kamiokande Collaboration), Phys. Rev. Lett. **110** 181802 (2013).
- [13] D.S. Ayers et al. (NOvA Collaboration), NOvA Technical Design Report, October 2007.

- [14] A. Norman, “Status of NO ν A”, talk at the XXIVth International Conference on Neutrino Physics and Astrophysics (Neutrino 2014), June 2014.
- [15] K. Abe et al. (T2K Collaboration), submitted to PTEP, arXiv:1409.7469

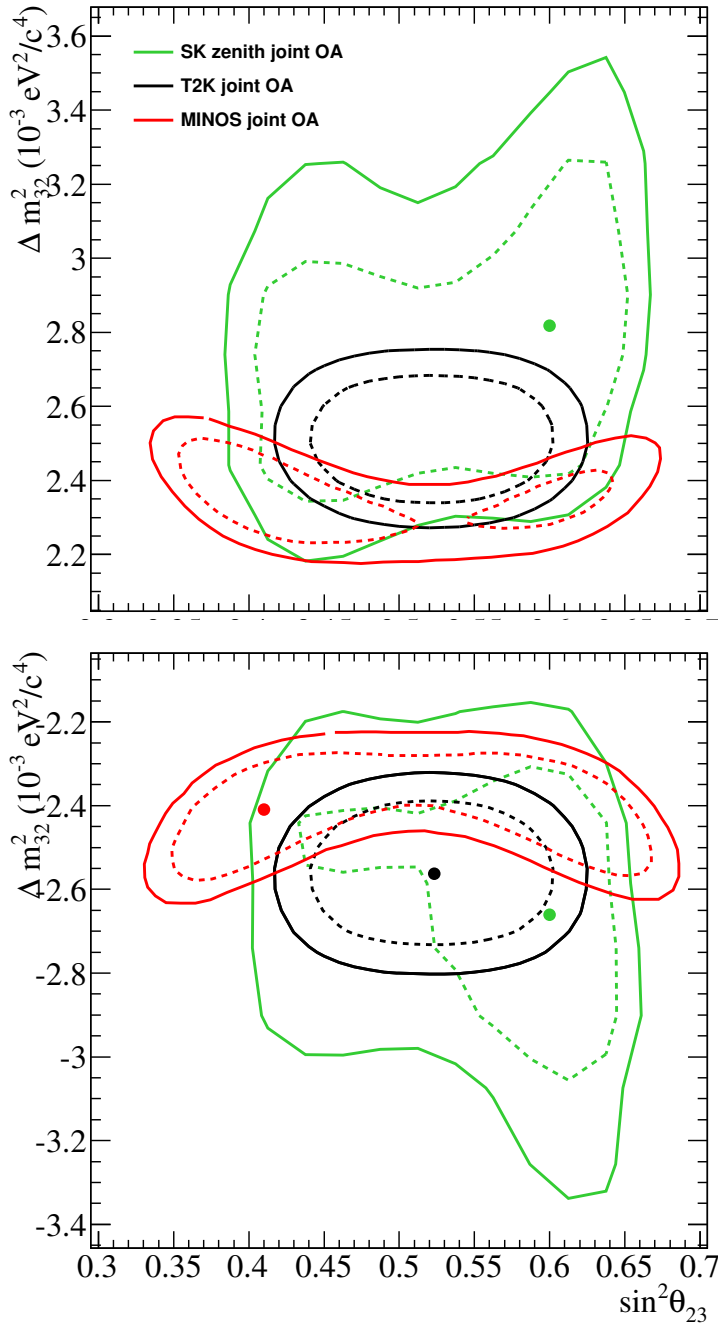


Figure 2: This figure compares the allowed regions from T2K, MINOS, and Super-Kamiokande. The top plot shows the fits for normal hierarchy, while the bottom plots shows fits for the inverted hierarchy. The solid (dashed) contours are the 90% (68%) CL regions. Constraints from reactor experiments are not included here.

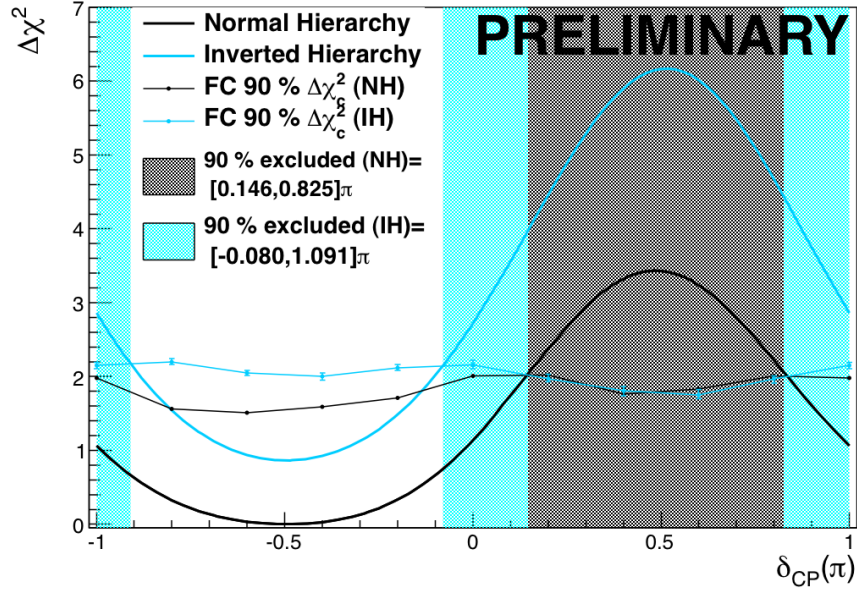


Figure 3: This figure shows the $\Delta\chi^2$ as a function of δ_{CP} for the T2K including constraints from reactor anti-neutrino disappearance measurements.

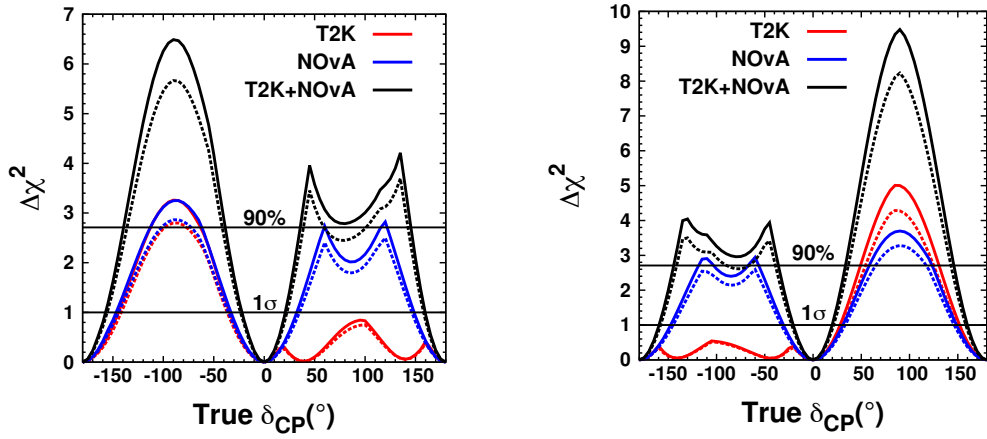


Figure 4: This figure shows the $\Delta\chi^2$ as a function of δ_{CP} for future T2K and NOvA running, assuming an equal mixture of neutrinos and anti-neutrinos. The left (right) plot shows assumes a true normal (inverted) hierarchy. This figure is reproduced from [15].